Article

J. Biol. Regul. Homeost. Agents. 2023; 37(9): 5035–5052
https://doi.org/10.23812/j.biol.regul.homeost.agents.20233709.489

Antioxidant, Anti-Inflammatory, and Anxiolytic-*Like* Effects of *Urena sinuata* L.: *In Vitro*, *In Vivo*, and *In Silico* Studies

Hossam Kamli[1,†], Mehedi Hasan Bappi[2,†], Tawhida Islam[2], Rajib Hossain[2], MD Munnaf Hossen[3], Abdullah Al Faruq[4], João Arthur de Oliveira Borges[5], Isaac Moura Araújo[5], Ray Silva de Almeida[5], Henrique Douglas Melo Coutinho[5,*], Catarina Martins Tahim[6], Elaine Cristina Pereira Lucetti[6], Muhammad Torequl Islam[2,*]

[1]Department of Clinical Laboratory Sciences, College of Applied Medical Sciences, King Khalid University, 61421 Abha, Saudi Arabia
[2]Department of Pharmacy, Bangabandhu Sheikh Mujibur Rahman Science and Technology University, 8100 Gopalganj, Bangladesh
[3]Department of Immunology, Health Science Center, Shenzhen University, 518060 Shenzhen, Guangdong, China
[4]Department of Pharmacy, Southern University Bangladesh, 4210 Chattogram, Bangladesh
[5]Department of Biological Chemistry, Laboratory of Microbiology and Molecular Biology, Program of Post-Graduation in Molecular Bioprospection, Regional University of Cariri, Crato, CE 63105-000, Brazil
[6]CECAPE College, Juazeiro do Norte, São José CE 63024-015, Brazil
*Correspondence: hdmcoutinho@gmail.com (Henrique Douglas Melo Coutinho); dmt.islam@bsmrstu.edu.bd (Muhammad Torequl Islam)
[†]These authors contributed equally.
Published: 20 September 2023

Background: ***Urena sinuata*** **L. is a shrubby wild plant used for centuries in folk medicine to treat bronchitis, rheumatism, fever, and waist pain. It is evident that it possesses antioxidant, anti-diarrheal, anti-atherothrombotic, sedative, anxiolytic, and analgesic effects in various test systems.**

Objectives: The goal of this research was to evaluate the anti-inflammatory, antioxidant, and anxiolytic activity along with the preliminary phytochemical investigation of the ethanolic leaf extract of ***U. sinuata*** **(ELEUS). Additionally, we also performed an** ***in silico*** **study to see the possible anxiolytic effects of its previously reported phytochemicals.**

Methods: Scavenging methods for nitric oxide ($NO^{\bullet}$), 2,2-diphenyl-1-picrylhydrazyl (DPPH), and hydroxyl radical ($^{\bullet}OH$) were used to determine antioxidant activity. The egg albumin model was used to assess anti-inflammatory action, while the elevated plus maze tested anxiolytic activity in adult male ***Swiss*** **albino mice. For the latter case, the control group received vehicle (10 mL/kg), the standard group received diazepam (DZP: 2 mg/kg), and the test groups received ELEUS at 200 and 400 mg/kg. Additionally, both the test groups were combined with DZP 2 mg/kg. All these treatments were given via oral gavage. Finally, we performed an** ***in silico*** **study to check the possible interactions of its literature-claimed compounds with gamma-aminobutyric acid $(GABA)_A$ receptor subunits.**

Results: Findings suggest that the ELEUS exhibited significant ($p < 0.05$) concentration-dependent antioxidant and anti-inflammatory effects. The highest activity was observed at 100 µg/mL. In mice, the extract had an anxiolytic effect that was significant ($p < 0.05$) and was dose-dependent. ELEUS 200 and 400 mg/kg were seen to potentiate the anxiolytic activity of the standard drug DZP (2 mg/kg) significantly ($p < 0.05$). Quercetagetin-6,7-O-dimethylether-3′-β-D-gluco-pyranoside, quercetagetin-6,7-O-dimethylether-4′-β-D glucopyranoside, and quercetagetin-6,7-O-dimethylether-3-β-D-glucopyranosid of ***U. sinuata*** **showed better interaction capacity with the $GABA_A$ receptor protein (α_1, α_2, α_3, α_4, α_5, and α_6) than the standard drug (diazepam).**

Conclusions: ELEUS possesses many important phytochemical groups and exhibits concentration-dependent antioxidant and anti-inflammatory effects as well as dose-dependent anxiolytic effects. ***U. sinuata*** **may be a good source of plant-based therapeutically active lead compounds for inflammation, oxidative stress, neurological diseases, and disorders like anxiety.**

Keywords: *Urena sinuata*; oxidative stress; inflammation; anxiety; molecular docking study

Journal of
BIOLOGICAL REGULATORS
and Homeostatic Agents

Introduction

Oxidative stress occurs when the formation of reactive oxygen species (ROS) and their removal are out of balance. It is one of the leading causes of chronic inflammation in our bodies and various disorders [1]. Apoptosis, oxidative stress, neuroinflammation, and reduced neurogenesis are the major consequences developing of anxiety and related diseases in the brain [2].

On the other hand, anxiety is a multifaceted psychiatric condition with an unidentified etiology that affects multiple neurotransmitters in the brain [3]. Apart from the 'conventional' gamma-aminobutyric acid (GABA) ergic system, the serotonergic, endocannabinoid, opioidergic, glutamatergic, neurokinin, and cholinergic systems may be investigated as potential novel therapeutic targets. However, there is still an unmet need to discover and develop more effective anxiolytics with the highest safety [4]. A growing interest in phytomedicine among health practitioners and patients has been evident in a number of recent clinical cases [3]. *Urena sinuata* L. (Family: Malvaceae), also known as 'Kunjia' in Bangladesh, is an herbal remedy found in Bangladesh, India, and some other regions. *U. sinuata* is an erect subshrub that is up to 1–2 m tall. Leaves are 4 to 8 cm long, palmately deeply lobed with rounded sinuses (curves), downy gray pubescent, and have star-shaped hairs. Flowers are pinkish-violet and clustered, measuring approximately 1 cm across. The velvety fruit is coated in hooked bristles (http://www.flowersofindia.net/catalog/slides/Burr%20Mallow.html).

Traditionally, *U. sinuata* is used to treat various diseases, including bronchitis, anti-rheumatic, antipyretic [5], and waist pain [6]. Scientific evidence suggests that *U. sinuata* contains many phytochemicals, including carbohydrates and gum, glycosides, alkaloids, reducing sugars, steroids, and flavonoids [5,7]. Three flavonoids were extracted from the leaves of *U. sinuata*: quercetagetin-6,7-O-dimethylether-3′-β-D-gluco-pyranoside (Compound I), quercetagetin-6,7-O-dimethylether-4′-β-D glucopyranoside (Compound II), and quercetagetin-6,7-O-dimethylether-3-β-D-glucopyranoside (Compound III) (Fig. 1). A different study found that this medicinal plant contains a glycoside known as 6,7-di-O-methyl-quercetagetin-3-O-D-glucopyranoside dehydrate [8,9]. Although the biological effects of these isolated compounds are yet to be investigated, it is evident that *U. sinuata* possesses antioxidant [5], anti-diarrheal [10], clot lysis [7,11,12], insecticidal and repellent [13], sedative, anxiolytic, and analgesic [14] effects in various test systems.

In this study, the antioxidant and anti-inflammatory properties of the ethanolic leaf extract of *U. sinuata* are investigated in various *in vitro* test models. In addition, the anxiolytic effect of *U. sinuata* was checked through *in vivo* and *in silico* studies.

Materials and Methods

In Vitro Studies

Collection, Identification and Extraction of Plant Materials

In March–May 2013, leaves of *U. sinuata* were harvested in the Chittagong hill tracts (Chittagong, Bangladesh). A scientist at the Bangladesh Forest Research Institute (BFRI) in Chittagong recognized the plant. The plant sample was deposited as a voucher specimen (BFRIH-2309). The leaves were then rinsed correctly in running water, dried in the shade (at a temperature below 45 °C), and ground into a coarse powder using a suitable grinder. 500 g of powdered materials were steeped in 97% ethanol for 20 days, with manual stirring occasionally. The yield of the air-dried (at room temperature) was 5.4% w/w. Until the test, the blackish ethanolic leaf extract of *U. sinuata* (ELEUS) was kept at 40 °C in an amber-colored glass vial.

Reagents and Chemicals

Zenith Pharmaceuticals Ltd., Bangladesh, generously gave diazepam (DZP), diclofenac sodium (DICLO-Na), and ascorbic acid (AA). For the investigation, ethanol (Merck, Darmstadt, Germany) was acquired. Analytical-grade chemicals and solvents were employed in this study.

Preliminary Phytochemical Study

The phytochemical groups in freshly produced ELEUS were qualitatively examined using established protocols, which included visual identification of distinctive color changes [15,16].

Total Phenolic Content (TPC) Assay

The Folin-Ciocalteau method is used to perform this test, which uses gallic acid as a standard [17]. In a 25-mL volumetric flask, 1 mL of the plant extract (1 mg/mL) was combined with 9 mL of distilled water. It was then given 2.5 mL of a 10-fold dilute Folin-Ciocalteau phenol reagent (1:10). After 5 minutes, 10 mL of a 7.5% Na_2CO_3 solution, followed by distilled water, was added to the mixture. The solution was then incubated at room temperature for 90 minutes in the dark. Gallic acid standard solutions (100, 125, 150, 175, and 200 µg/mL) were produced the same way as the extracts. A UV-visible spectrophotometer (UV-1900i, double-beam, Shimadzu, Kyoto, Japan) was used to measure the absorbances of the extract or standard solution against the reagent blank at 760 nm (UV-1800, Shimadzu, Kyoto, Japan). TPC content was calculated using a standard curve and represented as milligrams (mg) of gallic acid for every gram of extract.

Total Flavonoid Content (TFC) Assay

The aluminium chloride ($AlCl_3$) colorimetric assay was used for this test [18]. In a 10-mL volumetric flask, 1 mL of the extract (1 mg/mL) was combined with 4 mL of distilled water. The flask was filled with 0.30 mL of 5%

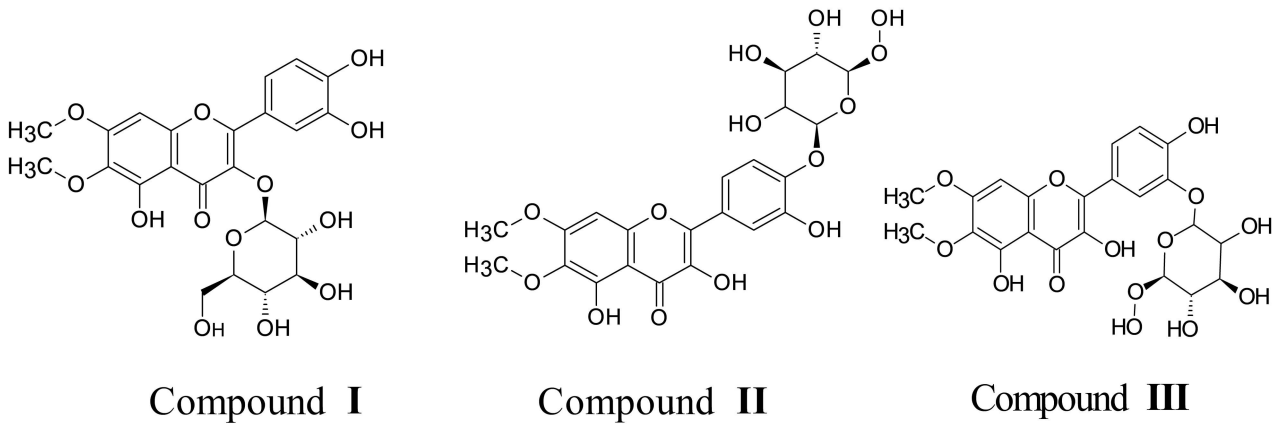

Fig. 1. Chemical compounds of *Urena sinuata* L.

sodium nitrite. Following 5 minutes, 0.30 mL of a 10% $AlCl_3$ solution was added to the mixture, followed by 2 mL of 1.0 M NaOH and distilled water. In the same way the extract was made, standard solutions of quercetin (20, 40, 60, 80, and 100 g/mL) were made. A UV-visible spectrophotometer (UV-1900i, double-beam, Shimadzu, Japan) was used to compare the absorbance of the extract and standard solutions to the reagent blank at 510 nm. The TFC was calculated using the calibration curve and is measured in milligrams (mg) of quercetin equivalent per gram of extract.

Test for Antioxidant Activity

2,2-Diphenyl-1-Picrylhydrazyl (DPPH) Test

The procedure given by Manzocco *et al.* (1998) [19] was used with minor modifications for this test. In a 2.7 mL ethanolic solution of DPPH, 0.3 mL of the sample at varied concentrations (20, 40, 60, 80, and 100 g/mL) was added (0.5 mM). The absorbance was measured at 517 nm with a spectrophotometer (UV-1900i, double-beam, Shimadzu, Japan) after 30 minutes. The positive control had a similar concentration of ascorbic acid (AA), while the control (vehicle) group received only 0.3 mL of vehicle (ethanol) added to the DPPH solution. The following formula was used to compute the DPPH radical scavenging potential:

$$\%\ \text{Inhibition of DPPH}^{\bullet}\ \text{scavenging} = [(Abr - Aar)/Abr] \times 100 \quad (1)$$

where, the absorbance of DPPH free radicals before and after the reaction is represented by A_{br} and A_{ar}, respectively. Half-minimal inhibitory concentration (IC_{50}) values for the test and standard were determined using non-linear regression analysis using the software below.

Nitric Oxide ($NO^{\bullet}$) Radical Scavenging Test

In a nutshell, 0.375 mL of the test sample (ELEUS/AA) was mixed with 1.5 mL sodium nitroprusside (10 mM) and 0.375 mL PBS in a 1.5 mL flask (pH 7.4). At 546 nm, the absorbance (A_{br}) was measured. 1 mL of the solution was combined with 1 mL of Griess reagent after incubating the reaction mixture at 37 °C for 1 hour. After 30 minutes of room temperature incubation, the reaction mixture's final absorbance (A_{ar}) was measured at 546 nm. The ethanol concentration in the control (vehicle) group was only 0.375 mL [20]. The following equation was used to compute the quantity of NO• inhibition:

$$\%\ \text{Scavenged NO}^{\bullet} = [(Abr - Aar)/Abr] \times 100 \quad (2)$$

where, the absorbance of $NO^{\bullet}$ free radicals before and after the reaction with the Griess reagent are A_{br} and A_{ar}, respectively. The IC_{50} values were also determined, as mentioned in the above-mentioned test.

Hydroxyl Radical ($^{\bullet}OH$) Scavenging Test

The test samples' ability to scavenge $^{\bullet}OH$ was assessed using the method outlined by Ruch *et al.* (1989) [21]. In phosphate buffer, a solution of 40 mM H_2O_2 was produced (50 mM; pH 7.4). By analyzing the absorbance at 230 nm, the quantity of H_2O_2 was determined spectrophotometrically. After 10 minutes, the test sample or standard (20 to 100 g/mL) was added to the H_2O_2, and the absorbance at 230 nm was measured. The following equation was used to compute the percentage of $^{\bullet}OH$ scavenging:

$$\%\ \text{OH scavenged} = [(A0 - A)/A0] \times 100 \quad (3)$$

where, the absorbance of the control sample/standard is A_0, while the absorbance of the test sample/standard is A. The IC_{50} values were also determined, as mentioned in the above-mentioned test.

Anti-Inflammatory Test (Egg Albumin Model)

The approach outlined by Sakat *et al.* (2010) [22] was used to conduct this test. In a nutshell, the reaction mixture (5 mL) contains 0.2 mL of egg albumin (from a fresh hen's egg), 2.8 mL of phosphate-buffered saline (pH: 6.4), and 2

Journal of
BIOLOGICAL REGULATORS
and Homeostatic Agents

mL of ELEUS or DICLO-Na at various concentrations. An equivalent volume of ethanol was used as a control. The mixtures were heated at 70 °C for 5 minutes after being incubated at 37 ± 2 °C for 15 minutes in an incubator. The optical density was measured at 660 nm after cooling, using the reagent as a blank using a colorimeter (AE-11M, Wincon Co., Ltd., Hunan, China). The following formula was used to compute the percentage inhibition of protein denaturation:

$$\% \text{ inhibition } = 100 - [(AControl - ATest)/ AControl] \times 100 \quad (4)$$

The half-maximal effective concentration (EC_{50}) values for the test and standard were determined using nonlinear regression analysis using the below-mentioned software GraphPad Prism (version 9.5, Insightful Science, La Jolla, CA, USA, accessed on 10 June 2022).

Acute Toxicity Study and Dose Determination

The test dose for this study of ELEUS was selected by the acute toxicity study following the OECD guidelines using *Swiss* albino mice [23]. Briefly, the ELEUS was administered orally at 500, 1000, and 2000 mg/kg doses. The animals were then frequently observed for behavioral changes, toxicological symptoms, and death for 2 days [24]. The animals' source and other necessary details have been provided under Experimental Animals of *In Vitro* Study section.

In Vivo Study

Experimental Animals

Adult *Swiss* albino male mice (25–35 g b.w., 5–6 weeks old) were purchased from the animal research branch of the Bangladesh Council of Scientific and Industrial Research (BCSIR), Chittagong, and acclimatized for 4 days at 25 ± 1 °C (relative humidity 55–60%) with a 12 h light/dark cycle. During this time, the animals were fed a BCSIR-recommended standard laboratory diet with access to unlimited water. After all test and analysis, the mices were euthanized by cervical dislocation.

Anxiolytic Activity Study

Elevated Plus Maze (EPM) Test

This experiment involved six groups of six animals per group. The first group was given the vehicle (0.5 percent tween 80 dissolved in 0.9 percent NaCl solution) (Control 10 mL/kg, p.o.), the second group was given DZP (2 mg/kg, i.p.), and the third and fourth groups were given ELEUS200 and ELEUS400 mg/kg, respectively (p.o.). After 30 minutes of administration of treatments, the animal was placed in the plus maze's center, with its nose pointing in the direction of one of the closed arms, and monitored for 5 minutes to calculate the following parameters: time spent in the open arms (TSOA), number of entries in the open arms (NEOA), and a total number of arm entries (TNAE). The equipment was cleansed with washing after each test, sanitized with 70% alcohol, and dried at room temperature. Additional groups of fifth and sixth animals were administered with ELEUS200 + DZP2 and ELEUS400 + DZP2, respectively. The metrics described were confirmed identically after 30 minutes of therapy.

Statistical Analysis

The mean and standard error of the mean (SEM) are used to calculate the results. GraphPad Prism (version 9.5, Insightful Science, La Jolla, CA, USA, accessed on 10 June 2022) was used to analyze the data, which included an analysis of variance (ANOVA) and a *t*-student's Newman-Keuls post hoc multiple comparison test with $p < 0.05$ at the 95% level of confidence [25]. Statistical (version 13.0, StatSoft Polska, Kraków, Poland, accessed on 7 January 2023) was also used to determine the correlation.

Molecular Docking (in Silico) Study

GABA Homology Model and Macromolecule

The *Swiss* model online server (https://swissmodel.expasy.org/interactive) was utilized to simulate gamma-aminobutyric acid (GABA) homology [26]. Prior to building the models, the sequence was retrieved from UniProt [27], and the template was chosen using BLAST analysis with the NCBI BLAST [28] tool. PROCHECK [29] was used to verify the Homology Model. The binding mechanism of GABA was investigated using molecular docking of QUR 3′-O-beta, QUR 4′-O-beta, QUR 3-O-beta, and DZP molecules.

Ligand Preparation

Prior to docking, we used the Swiss-PDB Viewer software tool (version 4.1.0, Swiss Institute of Bioinformatics, Biozentrum, Basel, accessed on 23 May 2021) to minimize the energy of the crystal structure. Furthermore, the chemical structures of quercetagetin-6,7-O-dimethylether-3′-β-D-gluco-pyranoside (QUR 3′-O-beta) (PubChem ID: 5748594), quercetagetin-6,7-O-dimethylether-4′-β-D glucopyranoside (QUR 4′-O-beta) (PubChem ID: 54758556), quercetagetin-6,7-O-dimethylether-3-β-D-glucopyranoside (QUR 3-O-beta) (PubChem ID: 5280804), and diazepam (DZP) (PubChem ID: 3016) have been published. Chem3D Pro21.0 (PerkinElmer Informatics, Inc., Waltham, MA, USA, accessed on 29 April 2022) software packages were used to optimize all ligand internal energies [30].

Docking Protocol

Computing docking research simulation is a computerized tool for drug design in drug discovery. The PyRx-virtual assessment tool (version 0.8, Scripps Research, San Diego, CA, USA, accessed on 7 September 2022) is used to examine the pharmacodynamic features of an active drug (ligand) by analyzing and putting molecules at specific

Table 1. Free radical scavenging capacity of the test sample and controls.

Parameter	DPPH test		NO• scavenging test		•OH scavenging test	
Conc. (µg/mL)	AA	ELEUS	AA	ELEUS	AA	ELEUS
20	61.67 ± 0.13*	43.15 ± 0.18*	54.51 ± 0.39*	31.01 ± 0.10*	59.19 ± 0.96*	39.09 ± 0.15*
40	71.78 ± 0.48*	59.23 ± 0.32*	59.24 ± 0.08*	39.06 ± 0.18*	63.11 ± 0.09*	45.23 ± 0.92*
60	77.81 ± 0.19*	67.31 ± 0.28*	69.23 ± 0.11*	44.59 ± 1.06*	68.25 ± 0.16*	62.61 ± 0.98*
80	81.89 ± 1.08*	79.19 ± 0.31*	74.24 ± 0.65*	60.04 ± 0.38*	79.23 ± 0.12*	69.21 ± 0.34*
100	88.11 ± 0.11*	82.09 ± 0.78*	84.29 ± 0.28*	75.15 ± 0.87*	89.11 ± 0.36*	78.54 ± 0.29*
IC_{50} (µg/mL)	10.87 ± 0.26	29.85 ± 0.35	13.38 ± 0.37	70.74 ± 0.53	12.09 ± 0.42	53.42 ± 0.44
CI (µg/mL)	5.28 to 22.36	22.77 to 40.86	4.26 to 42.00	55.00 to 77.17	2.43 to 60.25	42.08 to 65.40
R^2	0.92	0.93	0.80	0.77	0.71	0.85
Control	1.87 ± 0.21		2.08 ± 0.08		2.11 ± 0.96	

Values are mean ± SEM (n = 5); ANOVA followed by *t*-student's Newman–Keuls post hoc test; *$p < 0.05$ when compared to the Control (vehicle); ELEUS, ethanolic leaf extract of *Urena sinuata*; IC_{50}, half-minimal inhibitory concentration; CI, confidence of interval; R^2, coefficient of determination; DPPH, 2,2-diphenyl-1-picrylhydrazyl; NO•, nitric oxide; •OH, hydroxyl radical; ANOVA, analysis of variance; AA, ascorbic acid; SEM, standard error of the mean.

binding sites [31]. The docking results determine the degree ligands attach to a target molecule's catalytic site. The properties of the ligands in the original target protein grids [32] are investigated using Pymol Edu (version 1.7.4.5, Schrödinger, Inc., New York, USA, accessed on 2 July 2022) and BIOVIA Discovery Studio (version 21.1.0, Dassault Systemes, San Diego, CA, USA, accessed on 22 May 2021) for these active binding areas of the target protein [33–35].

Results

In Vitro Studies

Free Radical Scavenging Capacity

The preliminary phytochemical study suggests that ELEUS contains alkaloids, glycosides, steroids, flavonoids, reducing sugars, and gums. The TPC and TFC of the ELEUS were 52.37 ± 0.83 mg gallic acid/g and 139.10 ± 0.17 mg quercetin/g, respectively.

Both ELEUS and AA scavenged DPPH radicals in a concentration-dependent manner. The scavenging capacity is significant compared to the control group ($p < 0.05$). The highest DPPH scavenging capacity was recorded at 100 µg/mL of AA and ELEUS. Similarly, ELEUS and AA also exhibited •OH and NO• scavenging capacities. The calculated half-maximal inhibitory concentration (IC_{50}) of ELEUS for the DPPH, •OH, and NO• scavenging capacities are 29.85 ± 0.35, 53.42 ± 0.44, and 70.74 ± 0.53 µg/mL, respectively (Table 1).

All methods of determining antioxidant activity showed a high correlation of 0.930–0.961 (Table 2; Fig. 2).

ELEUS at all test concentrations (20–100 µg/mL) significantly ($p < 0.05$) inhibited heat-induced egg albumin denaturation, where the highest inhibition was seen at 100 µg/mL (59.29 ± 0.39). ELEUS markedly ($p < 0.05$) decreased heat-induced egg albumin denaturation at all test concentrations (20–100 µg/mL), with the maximum inhibition reported at 100 µg/mL (59.29 ± 0.39). DICLO-Na exhibited a better protein denaturation inhibitory effect at all concentrations. The EC_{50} calculated for DICLO-Na and ELEUS are 61.14 ± 0.57 and 70.10 ± 1.01 µg/mL, respectively. Control exhibited negligible anti-inflammatory effects (Table 3).

Table 2. Correlation matrix of different antioxidant assays.

Scavenging test	DPPH	NO•	•OH
DPPH			
NO•	0.930*		
•OH	0.961*	0.930*	

*$p < 0.05$.

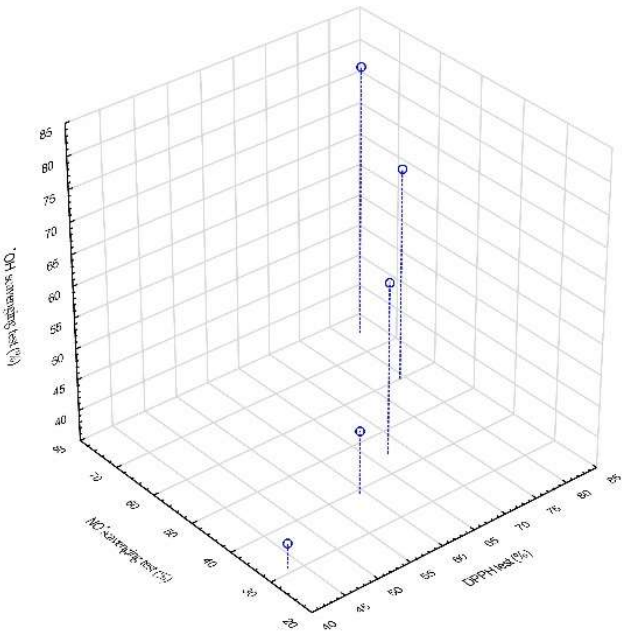

Fig. 2. 3D spread of scavenging tests (•OH versus DPPH and NO• scavenging tests).

Journal of
BIOLOGICAL REGULATORS
and Homeostatic Agents

Table 3. Protein denaturation inhibition capacity of the test sample and controls.

Treatments		Percentage inhibition of protein denaturation		EC_{50} (µg/mL) [CI (µg/mL); R^2]
		DICLO-Na	ELEUS	
Conc. (µg/mL)	20	29.13 ± 0.67*	9.13 ± 1.08*	DICLO-Na: 61.14 ± 0.57 [40.62 to 70.30; 0.80]; ELEUS: 70.10 ± 1.01 [51.68 to 76.85; 0.93]
	40	35.19 ± 0.58*	16.14 ± 0.96*	
	60	49.09 ± 0.28*	29.31 ± 0.78*	
	80	60.23 ± 1.08*	46.58 ± 0.62*	
	100	80.19 ± 0.48*	59.29 ± 0.39*	
Control		3.96 ± 0.31		-

Values are mean ± SEM (n = 5); ANOVA followed by *t*-student's *Newman–Keuls* post hoc test; *$p < 0.05$ when compared to the control (vehicle); DICLO-Na, diclofenac sodium; ELEUS, ethanolic leaf extract of *Urena sinuata*; EC_{50}, half-maximal effective concentration; CI, confidence of interval; R^2, coefficient of determination.

Table 4. Anxiolytic-*like* effects of the test sample and controls.

Treatments	TSOA (sec)	NEOA	TNAE
Control (10 mL/kg, p.o.)	123.7 ± 6.37	11.63 ± 0.74	27.00 ± 0.67
DZP (2 mg/kg, i.p.)	209.3 ± 3.53*^{b}	14.73 ± 0.58*	46.27 ± 0.54*^{bc}
ELEUS (200 mg/kg, p.o.)	203.3 ± 7.58*	16.67 ± 0.65*	39.14 ± 0.78*
ELEUS (400 mg/kg, p.o.)	207.3 ± 2.10*	14.77 ± 0.74*	41.44 ± 0.39*
ELEUS200 + DZP2	206.3 ± 3.08*^{c}	15.67 ± 0.65*	46.17 ± 0.53*^{bc}
ELEUS400 + DZP2	208.3 ± 2.00*^{c}	14.77 ± 0.74*	49.43 ± 0.17*^{abc}

Values are mean ± SEM (n = 6); ANOVA followed by *t*-student's *Newman–Keuls* post hoc test; *$p < 0.05$ when compared to the control (vehicle: 0.5% tween 80 dissolved in 0.9% NaCl solution); $^{a}p < 0.05$ when compared to the DZP group; $^{b}p < 0.05$ when compared to the ELEUS200, $^{c}p < 0.05$ when compared to the ELEUS400; TSOA, time spent in the open arms; NEOA, number of entries in the open arms; TNAE, total number of arm entries; DZP, diazepam; ELEUS, ethanolic leaf extract of *Urena sinuata*.

In Vivo Study

Acute Toxicity and Anxiolytic Activity

No significant behavioral changes, toxicity, or mortality were observed up to a 2000 mg/kg oral dose in the acute toxicity study in animals. Therefore, we selected the highest test dose of 400 mg/kg (15th of 2000 mg/kg) as the oral dose and its half-reduced dose of 200 as the lower dose for the present study. In the anxiolytic study, ELEUS at 200 and 400 mg/kg significantly ($p < 0.05$) increased the time spent in the open arms (TSOA), number of entries in the open arms (NEOA), and total number of arm entries (TNAE) as compared to the control group. The standard drug DZP2 also increased all these parameters significantly ($p < 0.05$) compared to the control group. ELEUS400 mg/kg produced a DZP-like effect in animals. Interestingly, ELEUS400 mg/kg, when co-treated with DZP (2 mg/kg), showed better activity in test animals. ELEUS400 + DZP2 group significantly ($p < 0.05$) increased the number of entries and time spent in open arms compared to their individual groups. This group showed similar behavior to the DZP2 group (Table 4).

Table 4 also suggests that both ELEUS doses significantly ($p < 0.05$) increased the total number of arm entries (TNAE) in comparison to the control group. ELEUS200 co-treated with the DZP2 was found to show an almost similar TNAE to that of the DZP2 group, while ELEUS400 co-treated with the DZP2 exhibited better effects than the other groups.

In Silico Studies

GABA Homology Model

Homology modeling has grown into a potent structural biology tool, dramatically decreasing the gap between empirically reported protein structures and identified protein sequences [36]. The Uniprot amino acid sequence of GABA (α_1, α_2, α_3, α_4, α_5, and α_6) collected by UNIPROT (Uniprot accession ID: P14867, P47869, P34903, P48169, P31644, and Q16445, respectively) was submitted to the NCBI Blast Programs, and the best homologous template's homology models for GABA (α_1, α_2, α_3, α_4, α_5, and α_6) were constructed using the Swiss model. Fig. 3 illustrates a 3D homology model of GABA receptors. The Swiss-PDB View software program (version 4.1.0) was used to optimize the GABA models prior to docking, and the Ramachandran plot was generated using PROCHECK to validate these GABA homology models, as shown in Fig. 4.

The Ramachandran plot is a simple approach for observing the distribution of torsion angles in a protein struc-

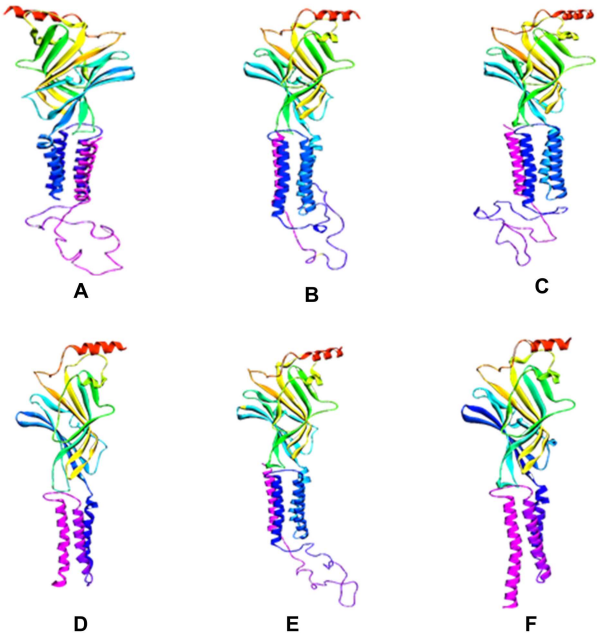

Fig. 3. Homology modeling of GABA receptors (A) α_1, (B) α_2, (C) α_3, (D) α_4, (E) α_5, & (F) α_6 through the Swiss model. GABA, gamma-aminobutyric acid.

ture. It also gives an overview of the permissible and banned ranges of torsion angle values, which is useful for determining the structural integrity of protein three-dimensional structures. The Ramachandran plot shows all of the structure's phi-psi torsion orientations (except those at the chain termini). Glycine residues are shown as triangles since they are not limited to the plot regions designated for one of the other side chain variants. The plot's coloring or shading indicates numerous locations: The darkest portions (in red) correlate to the "core" regions, which indicate the most advantageous phi-psi value combinations. In an ideal world, these "core" pieces would have held over 90% of the leftovers. One of the greatest indicators of stereochemical integrity is the percentage of residues in "core" sites (Fig. 4). According to Ramachandran plot statistics, residues in the most favored areas are around 93.86%, 93.80%, 91.35%, 95.77%, 92.61%, and 90.60% for GABA α_1, α_2, α_3, α_4,α_5, and α_6.

Interaction of QUR 3′-O-Beta with GABA Receptor

QUR 3′-O-beta binds to GABA receptor subunits α_1, α_2, α_3, α_4,α_5, and α_6 with affinities of –8.0, –8.2, –9.0, –7.5, –8.5, and –7.8 kcal/mol, respectively. Table 5 and Fig. 5A–F depict the 2D and 3D structures of QUR 3′-O-beta non-bond interactions with GABA receptor subunits.

Interaction of QUR 4′-O-Beta with GABA Receptor

QUR 4′-O-beta binds to GABA receptor subunits α_1, α_2, α_3, α_4, α_5, and α_6 with affinities of –7.9, –7.6, –7.7, –7.4, –8.2 and –7.4 kcal/mol, respectively. Table 5 and Fig. 5G–L depict the 2D and 3D structures of QUR 4′-O-beta non-bond interactions with GABA receptor subunits.

Interaction of QUR 3-O-Beta with GABA Receptor

QUR 3-O-beta binds to GABA receptor subunits α_1, α_2, α_3, α_4, α_5, and α_6 with affinities of –8.0, –7.9, –9.0, –7.3, –7.0 and –7.6 kcal/mol, respectively. Table 5 and Fig. 5M–R depicts the 2D and 3D structures of QUR 3-O-beta non-bond interactions with GABA receptor subunits.

Interaction of DZP with GABA Receptor

DZP binds to GABA receptor subunits α_1, α_2, α_3, α_4, α_5, and α_6 with affinities of –6.7, –6.8, –6.8, –7.1, –6.5, and –6.8 kcal/mol, respectively. Table 5 and Fig. 5S–X depict the 2D and 3D structures of DZP non-bond interactions with GABA receptor subunits.

Discussion

Our bodies' repair systems counteract cell damage and the cytogenetic changes it causes [37]. ROS causes damage to cell macromolecules such as proteins, carbohydrates, lipids, and genetic elements when present in high concentrations (e.g., RNA and DNA) [38]. Antioxidants from various sources, including plant-based antioxidants, may counteract these detrimental effects [39,40].

The DPPH test is a commonly used *in vitro* antioxidant capacity test that involves the reduction of stable DPPH free radicals by reducing compounds known as antioxidants [41,42]. On the other hand, $^{\bullet}$OH is a free radical with a relatively short half-life (about 9–10 seconds), which is reflected in its immunological effect. However, excessive OH generation can harm nearly all macromolecules, including nucleic acids (mutations), carbohydrates, lipids (lipid peroxidation), and amino acids (e.g., conversion of Phe to m-Tyr and o-Tyr). NO plays important biological functions, however, as it can diffuse freely across the membranes and cause lipid peroxidation. It has an important role in cardiovascular and neurological diseases [43,44]. An earlier report suggests that *U. sinuata* has free radical scavenging capacity; the authors determined the IC_{50} value for its chloroform extract at 10.64 µg/mL [5]. Our study demonstrates that ELEUS showed a concentration-dependent DPPH, $^{\bullet}$OH, and NO$^{\bullet}$ scavenging capacity where the IC_{50}values were 29.85 ± 0.35, 53.42 ± 0.44, and 70.74 ± 0.53 µg/mL, respectively. It seems chloroform extract's DPPH radical scavenging capacity is better than its ethanolic extract's.

There is a relationship between excessive free radical production and oxidative stress, leading to an inflammatory reaction in our body. Certain medicinal components like flavonoids [45,46] and alkaloids [47] have antioxidant and anti-inflammatory capacities. Inflammation is a defensive response but can cause major health concerns, including neurologic diseases and disorders, depending on its in-

Journal of
BIOLOGICAL REGULATORS
and Homeostatic Agents

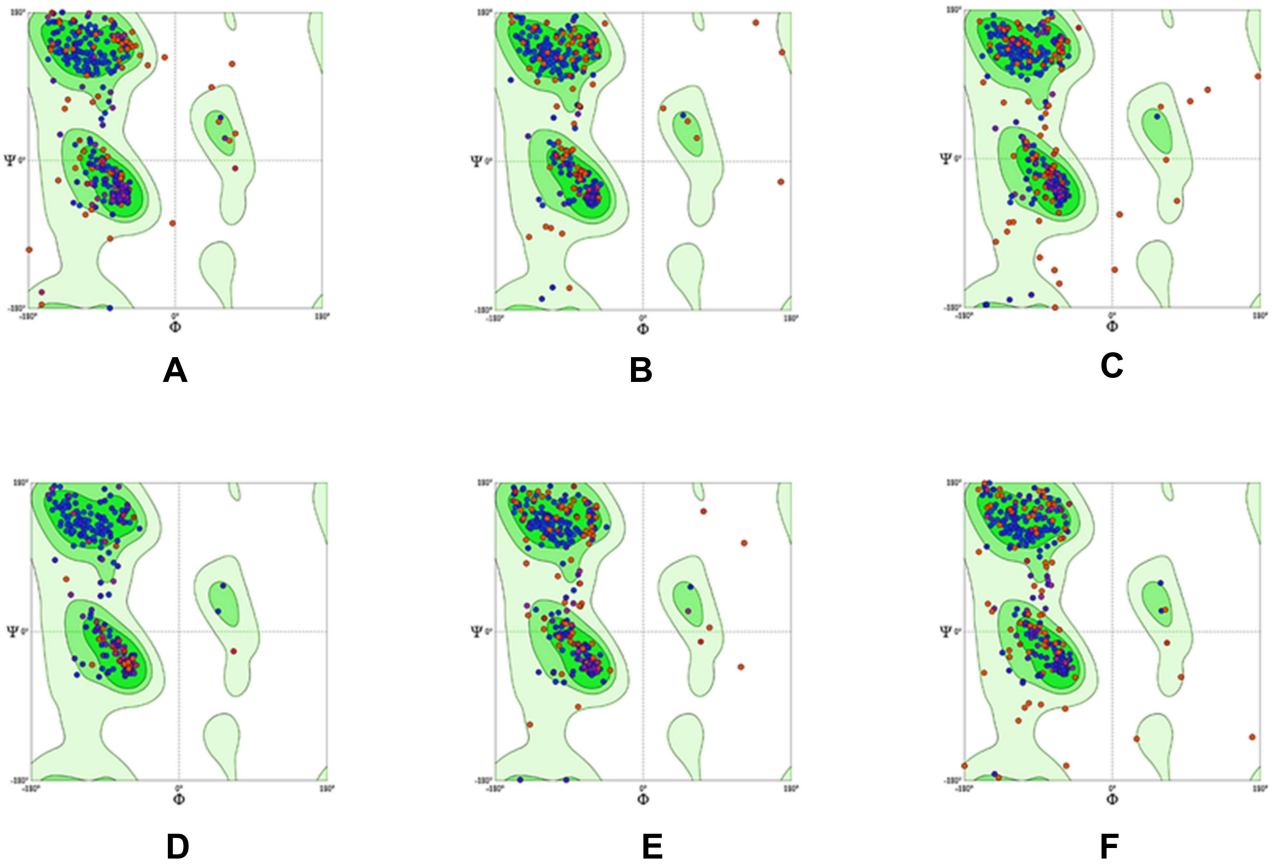

Fig. 4. Swiss model used to optimize the predictions of GABA receptors (A) α_1, (B) α_2, (C) α_3, (D) α_4, (E) α_5, and (F) α_6.

tensity [48]. In this study, the ELEUS demonstrated strong anti-inflammatory activity in egg albumin (*in vitro*) tested in a concentration-dependent manner. To our knowledge, *U. sinuata* underwent an anti-inflammatory test for the first time in our study.

Depression and anxiety are the most frequent emotional problems people face worldwide. Anxiety is a normal emotion that can become problematic if it occurs too frequently. Anxiety disorders affect more than 20% of the adult population worldwide at some point during their lives [14,49]. Anxiety disorders are linked to mental problems such as depression, stressful situations, and various physical ailments (e.g., endocrine disorders such as thyroid disorders and glucose metabolic disorders, for instance, hypoglycemia and diabetes). In treating anxiety disorders, benzodiazepines, selective serotonin reuptake inhibitors (SSRIs), and beta-adrenergic blocking medicines are widely utilized. On the other hand, these medicines are known to cause drug addiction and a variety of other side effects [50,51]. As a result, alternative drug research is critical for this reason. Anxiety disorders are caused by oxidative stress, or "sensor of distress", leading to neuroinflammation [52]. Our findings suggest that ELEUS exerted anxiolytic-*like* effects in *Swiss* mice. However, when we combined ELEUS with the standard drug DZP, it showed animal anxiolytic effects. DZP is a GABA/benzodiazepine receptor agonist with various adverse effects, such as tight muscles and depression [51,53]. The results observed in this study also agree with the findings of previous reports [12,54], where the chloroform extract of the plant leaf was found to exert an anxiolytic-*like* effect on test animals. Polyphenolic substances are protective in nature [55]. Flavonoids, on the other hand, have been shown to reduce the risk of various chronic diseases, including cardiovascular disease (CVD), cancer, and neurological disorders, when consumed regularly [56]. The present findings suggest that *U. sinuata* contains flavonoids. Moreover, the herb also contains significant amounts of TPC and TFC.

Bioinformatics, or computational analyses, are milestones in modern drug discovery and development. Many of these strategies are now popularly used in almost all branches of life sciences [57]. To date, numerous advanced molecular modeling software, extensive data analytical tools, and high-speed processing units have been introduced, which can be used in almost all fields of drug discovery, including neurological diseases and disorders [58].

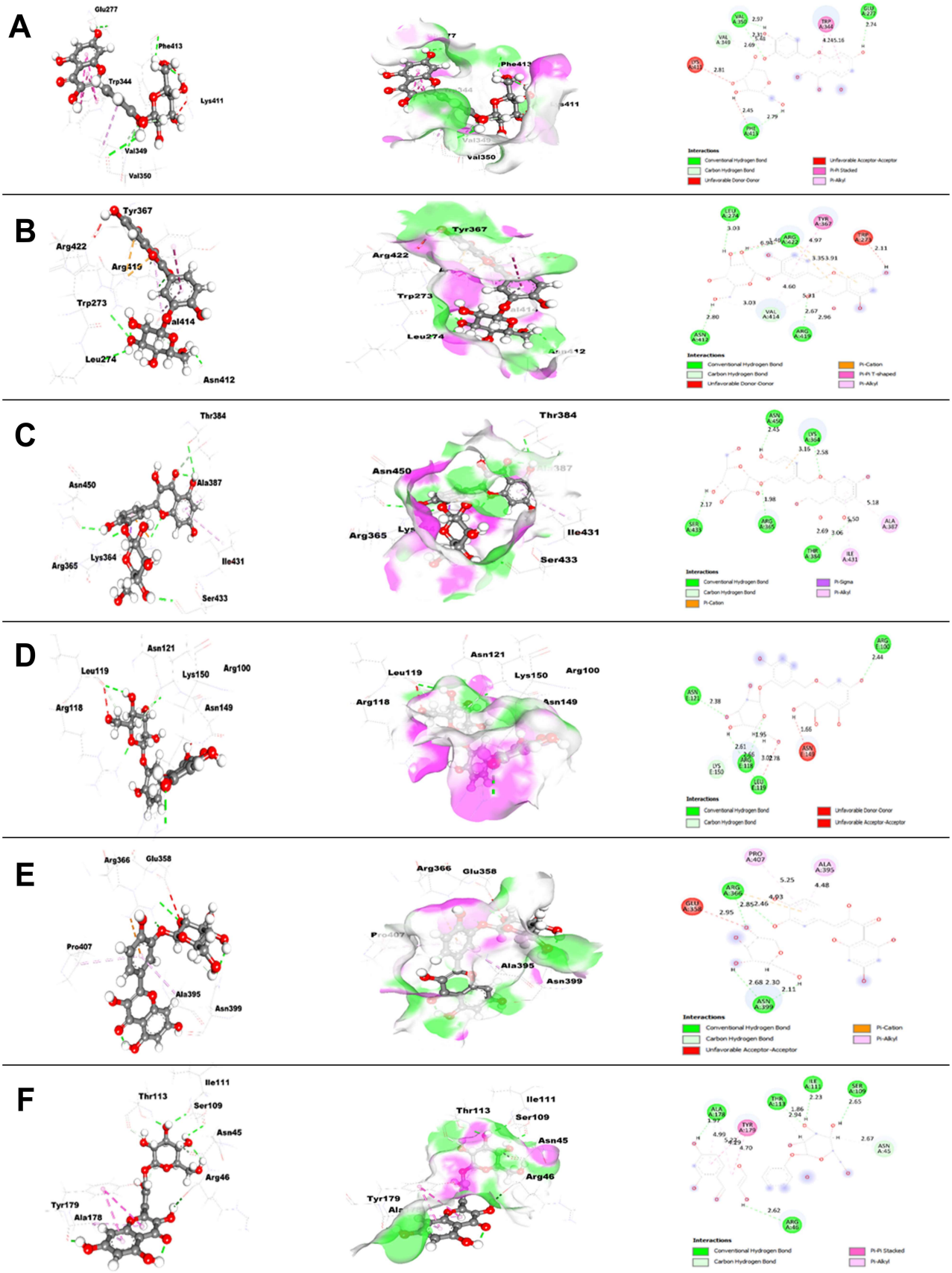
A
Glu277
Phe413
Trp344
Lys411
Val349
Val350
Interactions
Conventional Hydrogen Bond
Carbon Hydrogen Bond
Unfavorable Donor-Donor
Unfavorable Acceptor-Acceptor
Pi-Pi Stacked
Pi-Alkyl
B
Tyr367
Arg422
Arg419
Trp273
Val414
Leu274
Asn412
Interactions
Conventional Hydrogen Bond
Carbon Hydrogen Bond
Unfavorable Donor-Donor
Pi-Cation
Pi-Pi T-shaped
Pi-Alkyl
C
Thr384
Asn450
Ala387
Arg365
Lys364
Ile431
Ser433
Interactions
Conventional Hydrogen Bond
Carbon Hydrogen Bond
Pi-Cation
Pi-Sigma
Pi-Alkyl
D
Asn121
Leu119
Lys150
Arg100
Arg118
Asn149
Interactions
Conventional Hydrogen Bond
Carbon Hydrogen Bond
Unfavorable Donor-Donor
Unfavorable Acceptor-Acceptor
E
Arg366
Glu358
Pro407
Ala395
Asn399
Interactions
Conventional Hydrogen Bond
Carbon Hydrogen Bond
Unfavorable Acceptor-Acceptor
Pi-Cation
Pi-Alkyl
F
Ile111
Thr113
Ser109
Asn45
Arg46
Tyr179
Ala178
Interactions
Conventional Hydrogen Bond
Carbon Hydrogen Bond
Pi-Pi Stacked
Pi-Alkyl

Journal of
BIOLOGICAL REGULATORS
and Homeostatic Agents

G

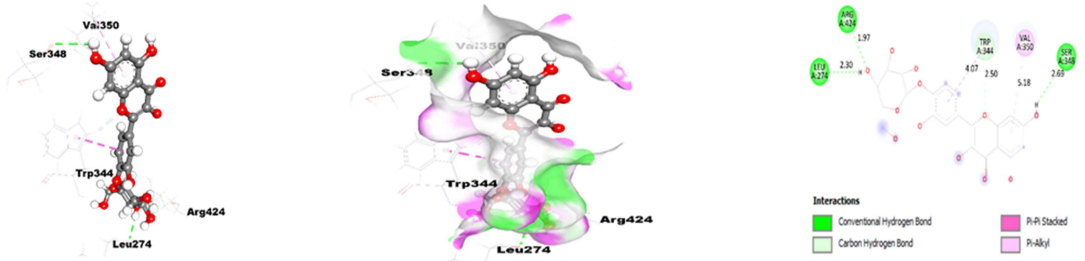

H

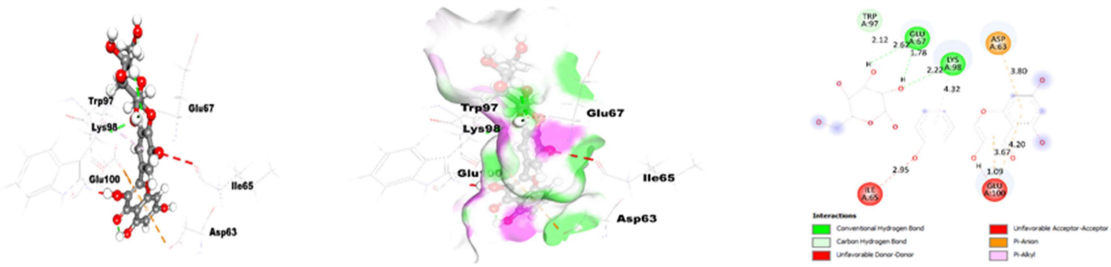

I

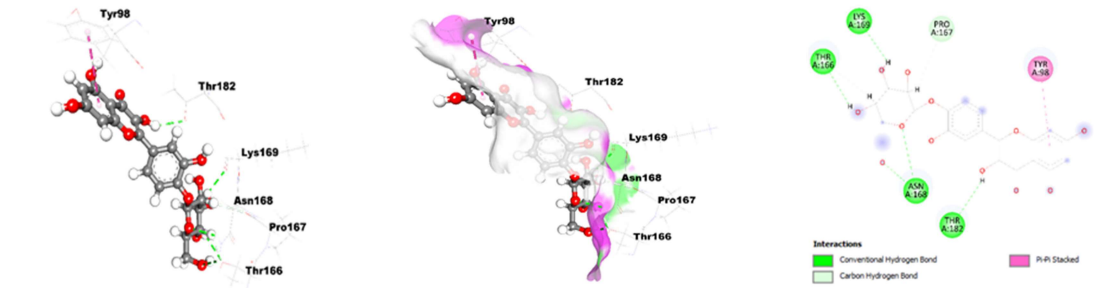

J

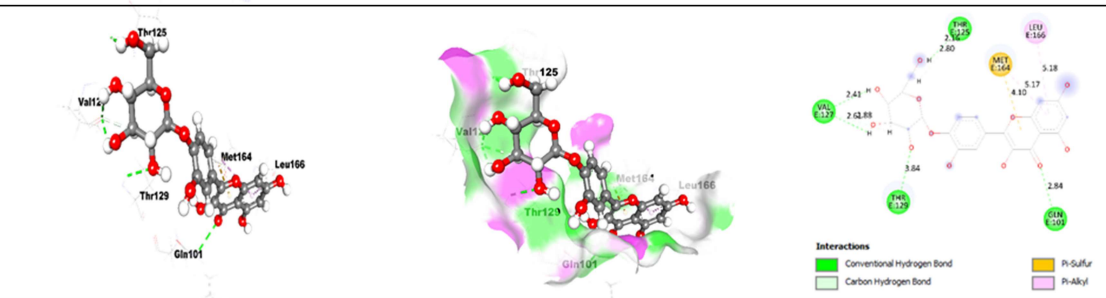

K

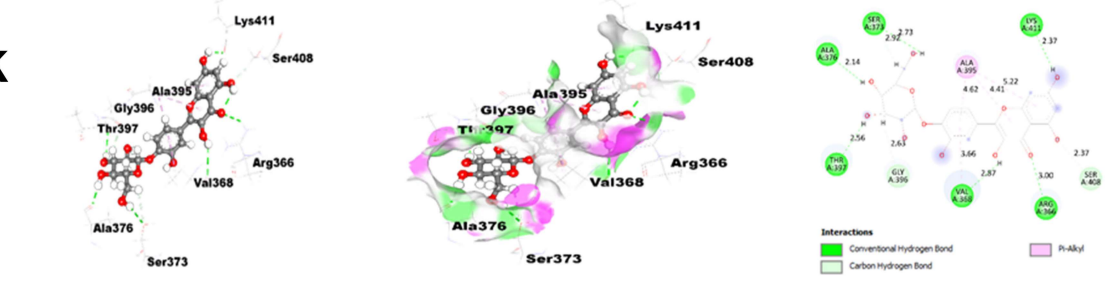

L

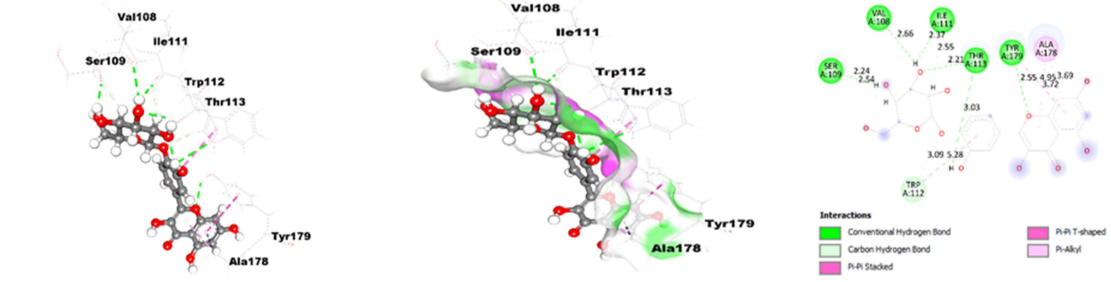

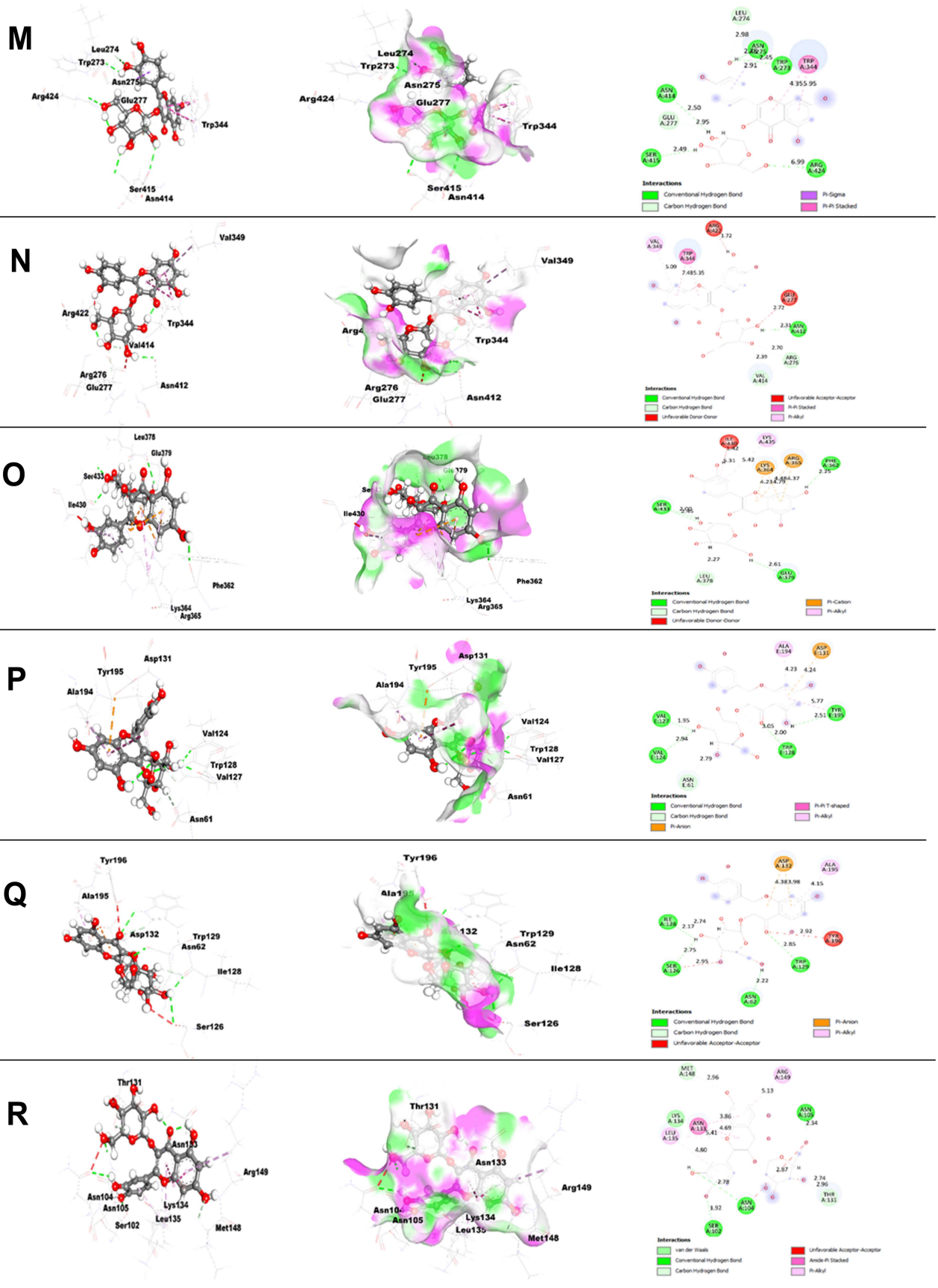
M
Leu274
Trp273
Asn275
Arg424
Glu277
Trp344
Ser415
Asn414
Interactions
Conventional Hydrogen Bond
Carbon Hydrogen Bond
Pi-Sigma
Pi-Pi Stacked
N
Val349
Arg422
Trp344
Val414
Arg276
Glu277
Asn412
Interactions
Conventional Hydrogen Bond
Carbon Hydrogen Bond
Unfavorable Donor-Donor
Unfavorable Acceptor-Acceptor
Pi-Pi Stacked
Pi-Alkyl
O
Leu378
Glu379
Ser433
Ile430
Phe362
Lys364
Arg365
Interactions
Conventional Hydrogen Bond
Carbon Hydrogen Bond
Unfavorable Donor-Donor
Pi-Cation
Pi-Alkyl
P
Asp131
Tyr195
Ala194
Val124
Trp128
Val127
Asn61
Interactions
Conventional Hydrogen Bond
Carbon Hydrogen Bond
Pi-Anion
Pi-Pi T-shaped
Pi-Alkyl
Q
Tyr196
Ala195
Asp132
Trp129
Asn62
Ile128
Ser126
Interactions
Conventional Hydrogen Bond
Carbon Hydrogen Bond
Unfavorable Acceptor-Acceptor
Pi-Anion
Pi-Alkyl
R
Thr131
Asn133
Arg149
Asn104
Asn105
Lys134
Ser102
Leu135
Met148
Interactions
van der Waals
Conventional Hydrogen Bond
Carbon Hydrogen Bond
Unfavorable Acceptor-Acceptor
Amide-Pi Stacked
Pi-Alkyl

Journal of
BIOLOGICAL REGULATORS
and Homeostatic Agents

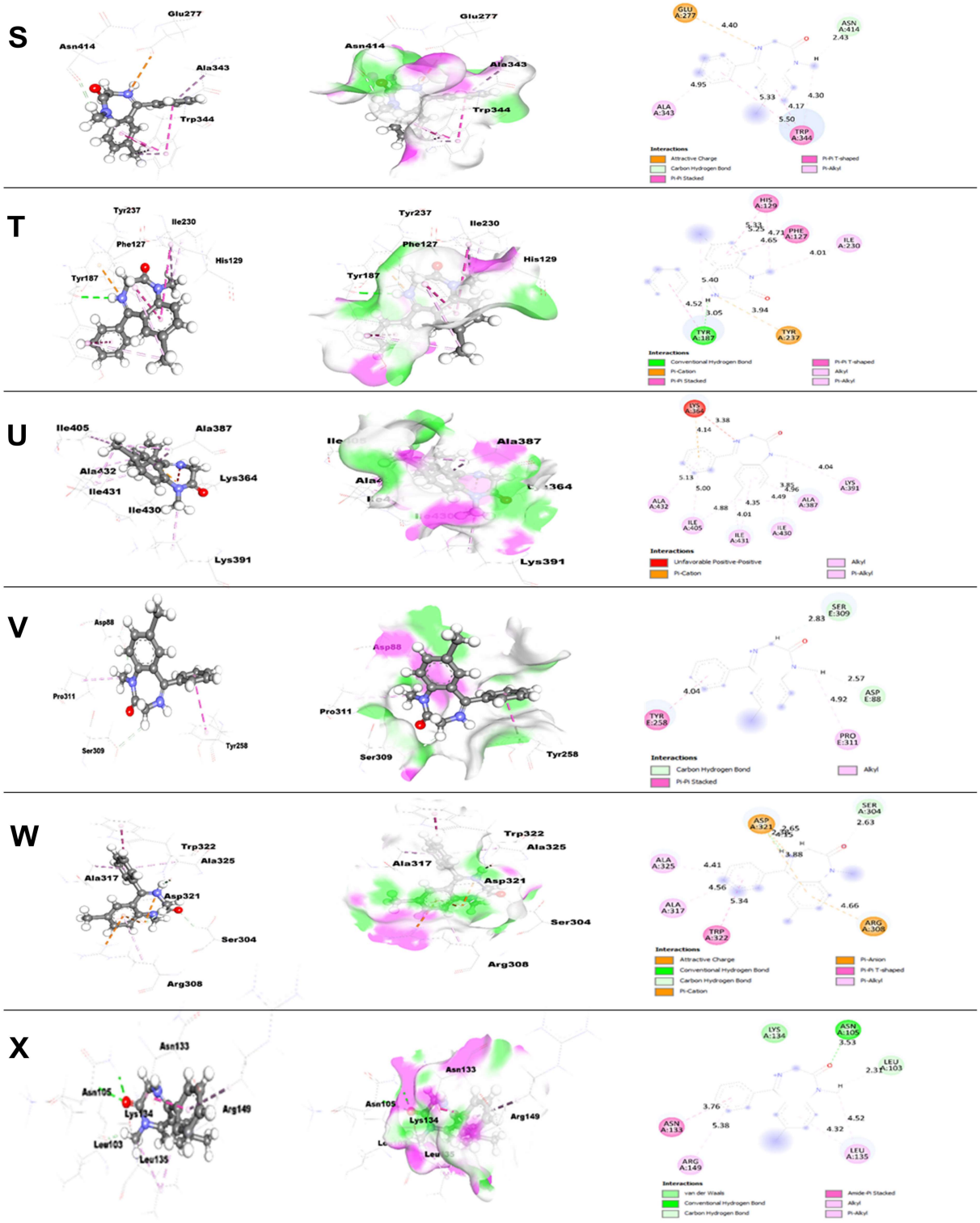

Fig. 5. The two-dimensional (2D) and three-dimensional (3D) structures of molecular docking contacts between (A) QUR 3′-O-beta & GABA-α_1 (B) QUR 3′-O-beta & GABA-α_2 (C) QUR 3′-O-beta & GABA-α_3 (D) QUR 3′-O-beta & GABA-α_4 (E) QUR 3′-O-beta & GABA-α_5 (F) QUR 3′-O-beta & GABA-α_6 (G) QUR 4′-O-beta & GABA-α_1 (H) QUR 4′-O-beta & GABA-α_2 (I) QUR 4′-O-beta & GABA-α_3 (J) QUR 4′-O-beta & GABA-α_4 (K) QUR 4′-O-beta & GABA-α_5 (L) QUR 4′-O-beta & GABA-α_6 (M) QUR 3-O-beta & GABA-α_1 (N) QUR 3-O-beta & GABA-α_2 (O) QUR 3-O-beta & GABA-α_3 (P) QUR 3-O-beta & GABA-α_4 (Q) QUR 3-O-beta & GABA-α_5 (R) QUR 3-O-beta & GABA-α_6 (S) DZP & GABA-α_1 (T) DZP & GABA-α_2 (U) DZP & GABA-α_3 (V) DZP & GABA-α_4 (W) DZP & GABA-α_5 (X) DZP & GABA-α_6.

Table 5. Best binding affinity values and non-bond interactions of quercetagetin-6,7-O-dimethylether -3′-β-D-gluco-pyranoside (QUR 3′-O-beta), quercetagetin-6,7-O-dimethylether-4′-β-D glucopyranosi-de (QUR 4′-O-beta), quercetagetin-6,7-O-dimethylether-3-β-D-glucopyranoside (QUR 3-O-beta), and diazepam (DZP) with GABA receptors.

Ligand and protein (receptor)	Binding affinity (kcal/mol)	H-bond		Hydrophobic bond		Other bonds [Electrostatic (E) or, Others (O)]	
		Residues	Bond types	Residues	Bond types	Residues	Bond types
(A) QUR 3′-O-beta & GABA-α_1	–8.0	Val350, Phe413, Glu277, Val350 Val349	Conventional Carbon hydrogen	Trp344, Trp344, Trp344 Val349	Pi-pi stacked Pi-Alkyl	-	
(B) QUR 3′-O-beta & GABA-α_2	–8.2	Arg419, Arg422, Arg422, Asn412, Leu274 Val414, Arg419 Arg422	Conventional Carbon hydrogen Pi-cation	Tyr367 Val414, Val414	Pi-pi T-shaped Pi-Alkyl	Arg422 Arg422	Pi-donor-H bond (E) Pi-cation (E)
(C) QUR 3′-O-beta & GABA-α_3	–9.0	Lys364, Arg365, Ser433, Thr384, Asn450 Thr384 Lys364	Conventional Carbon hydrogen Pi-cation	Lys364 Ala387, Ile431	Pi-sigma Pi-Alkyl	Lys364	Pi-donor-H bond (E)
(D) QUR 3′-O-beta & GABA-α_4	–7.5	Agr100, Agr118, Asn121, Leu119 Lys150, Leu119	Conventional Carbon hydrogen	-		-	
(E) QUR 3′-O-beta & GABA-α_5	–8.5	Arg366, Arg366, Asn399, Asn399 Asn399	Conventional Carbon hydrogen	Ala395, Pro407	Pi-Alkyl	Arg366	Pi-cation (E)
(F) QUR 3′-O-beta & GABA-α_6	–7.8	Thr113, Ser109, Ile111, Ala178, Arg46 Asn45, Thr113	Conventional Carbon hydrogen	Tyr179, Tyr179 Ala178, Ala178	Pi-pi stacked Pi-Alkyl	-	
(G) QUR 4′-O-beta & GABA-α_1	–7.9	Arg424, Leu274, Ser348 Trp244	Conventional Carbon hydrogen	Trp344 Val350	Pi-pi stacked Pi-Alkyl	-	
(H) QUR 4′-O-beta & GABA-α_2	–7.6	Lys98, Glu67, Glu67 Trp97	Conventional Carbon hydrogen	Lys98	Pi-Alkyl	Asp63, Glu100, Glu100	Pi-anion (E)
(I) QUR 4′-O-beta & GABA-α_3	–7.7	Asn168, Asn168, Thr166, Lys169, Thr182 Thr166, Pro167	Conventional Carbon hydrogen	Tyr98	Pi-pi stacked	-	

Table 5. Continued.

Ligand and protein (receptor)	Binding affinity (kcal/mol)	H-bond		Hydrophobic bond		Other bonds [Electrostatic (E) or, Others (O)]	
		Residues	Bond types	Residues	Bond types	Residues	Bond types
(J) QUR 4′-O-beta & GABA-α_4	–7.4	Gln101, Thr129, Thr129, Thr125, Val127, Val127 Val127, Thr125	Conventional Carbon hydrogen	Met164, Leu166	Pi-Alkyl	Met164	Pi-sulfur (O)
(K) QUR 4′-O-beta & GABA-α_5	–8.2	Arg366, Ser373, Ala376, Thr397, Lys411, Val368 Ser408, Gly396, Ser373	Conventional Carbon hydrogen	Val368, Ala395, Ala395, Ala395	Pi-Alkyl	-	
(L) QUR 4′-O-beta & GABA-α_6	–7.4	Thr113, Tyr179, Ser109, Val108, Ile111, Thr113 Trp112, Ser109, Ile111	Conventional Carbon hydrogen	Trp112 Tyr179 Ala178, Ala178	Pi-pi stacked Pi-pi T-shaped Pi-Alkyl	-	
(M) QUR 3-O-beta & GABA-α_1	–8.0	Asn275, Arg424, Arg424, Ser415, Asn414, Trp273 Leu274, Glu277	Conventional Carbon hydrogen	Trp344, Trp344, Trp344, Trp344 Asn275	Pi-pi stacked Pi-sigma	-	
(N) QUR 3-O-beta & GABA-α_2	–7.9	Asn412 Arg276, Val414	Conventional Carbon hydrogen	Trp344, Trp344, Trp344, Trp344 Val349	Pi-pi stacked Pi-Alkyl	-	
(O) QUR 3-O-beta & GABA-α_3	–9.0	Ser433, Glu379, Ser433, Phe362 Leu378	Conventional Carbon hydrogen	Ile430, Lys435, Lys364, Lys364	Pi-Alkyl	Lys364, Lys364, Arg365, Arg365	Pi-cation (E)
(P) QUR 3-O-beta & GABA-α_4	–7.3	Trp128, Val124, Val127, Tyr195 Trp128, Asn61	Conventional Carbon hydrogen	Tyr195 Ala194	Pi-pi T-shaped Pi-Alkyl	Asp131	Pi-anion (E)
(Q) QUR 3-O-beta & GABA-α_5	–7.0	Trp129, Asn62, Ser126, Ile128 Trp129, Ile128	Conventional Carbon hydrogen	Ala195	Pi-Alkyl	Asp132, Asp132	Pi-anion (E)
(R) QUR 3-O-beta & GABA-α_6	–7.6	Ser102, Asn105, Asn104 Thr131, Met148, Thr131	Conventional Carbon hydrogen	Leu135, Arg149, Leu135 Asn133; Lys134, Asn133; Lys134	Pi-Alkyl Amide-pi stacked	-	

Table 5. Continued.

Ligand and protein (receptor)	Binding affinity (kcal/mol)	H-bond		Hydrophobic bond		Other bonds [Electrostatic (E) or, Others (O)]	
		Residues	Bond types	Residues	Bond types	Residues	Bond types
(S) DZP & GABA-α_1	–6.7	Asn414	Carbon hydrogen	Trp344, Trp344 Trp344 Trp344, Trp344, Trp344, Ala343	Pi-pi stacked Pi-pi T-shaped Pi-Alkyl	Glu277	Attractive charge (E)
(T) DZP & GABA-α_2	–6.8	Tyr187	Conventional	Tyr187 Phe127 Ile230 Phe127, His129, Tyr187	Pi-pi stacked Pi-pi T-shaped Alkyl Pi-Alkyl	Tyr237	Pi-cation (E)
(U) DZP & GABA-α_3	–6.8	-		Ala387, Ile405, Ile431, Lys391, Ile430 Ile405, Ala432, Ala387	Alkyl Pi-Alkyl	Lys364	Pi-cation (E)
(V) DZP & GABA-α_4	–7.1	Asp88, Ser309	Carbon hydrogen	Tyr258 Pro311	Pi-pi stacked Alkyl	-	
(W) DZP & GABA-α_5	–6.5	Asp321 Ser304, Asp321	Conventional Carbon hydrogen	Trp322 Ala317, Ala325, Arg308	Pi-pi T-shaped Pi-Alkyl	Asp321 Arg308 Asp321	Attractive charge (E) Pi-cation (E) Pi-anion (E)
(X) DZP & GABA-α_6	–6.8	Asn105, Asn105 Leu103	Conventional Carbon hydrogen	Asn133; Lys134 Leu135 Arg149, Leu135	Amide-pi stacked Alkyl Pi-Alkyl	-	

Journal of
BIOLOGICAL REGULATORS
and Homeostatic Agents

In this study, ELEUS showed promising radical scavenging and *in vitro* anti-inflammatory capacities. Studies suggest that substances with these properties may play important roles in neuroprotection capacity [59,60]. Thus, the neuroprotective effect of ELEUS might be linked to its potent antioxidant and anti-inflammatory capacities. Natural compounds like alkaloids, glycosides, flavonoids, etc., have promising neuroprotective effects [61–65]. In this study, *in silico* studies suggest that compound-I showed strong interactions with GABA-α_3 and α_5 subunits, while compound-III showed strong interactions with GABA-α_3 subunits. Interestingly, all three compounds showed better interaction capacity with six GABA subunits than the standard DZP.

Conclusions

In summary, alkaloids, flavonoids, and glycosides are among the secondary metabolites found in ELEUS. In a concentration-dependent way, ELEUS showed promising antioxidant and anti-inflammatory properties. In *Swiss* albino mice, ELEUS produced an anxiolytic-*like* effect. ELEUS at 400 mg/kg was found to enhance DZP-mediated calming effects in experimental animals. Compound-I showed strong interactions with GABA-α_3 (–9.0 kcal/mol) and α_5 (–8.5 kcal/mol) subunits, while compound-III with GABA-α_3 (–9.0 kcal/mol) subunits. These three compounds showed better interaction capabilities with six subunits of GABA than the standard drug DZP. Thus, the anxiolytic-*like* effects of ELEUS or its combination with DZP might be due to synergistic effects and possibly through the GABA receptor interaction pathway. Therefore, ELEUS might be a good source of anti-anxiety agents. Additional research is needed to identify the other active chemicals responsible for each biological function and assess their mechanisms of action.

Availability of Data and Materials

All data and material will be available after a reasonable request to the corresponding author.

Author Contributions

Conceptualization, HK, HDMC, RSA and MTI; methodology, MHB, CMT, TI, JAOB and RH; investigation, MMH, IMA and AAF; writing—original draft preparation, IMA and JAOB; writing—review and editing, RSA and CMT; visualization, ECPL; supervision, HDMC and MTI; project administration, HDMC. All authors contributed to editorial changes in the manuscript. All authors read and approved the final manuscript. All authors have participated sufficiently in the work and agreed to be accountable for all aspects of the work.

Ethics Approval and Consent to Participate

This study was funded and approved by the Research Center, Bangabandhu Sheikh Mujibur Rahman Science and Technology University (BSMRSTU) (#2023-33).

Acknowledgment

Not applicable.

Funding

The authors extend their appreciation to the Deanship of Scientific Research at King Khalid University for funding this work through large group Research Project under grant number RGP2/362/44. The APC was funded by Ministry of Education and Science in Poland within the statutory activity of Medical University of Lublin (DS 25/2022).

Conflict of Interest

The authors declare no conflict of interest.

References

[1] Ansari MY, Ahmad N, Haqqi TM. Oxidative stress and inflammation in osteoarthritis pathogenesis: Role of polyphenols. Biomedicine & Pharmacotherapy. 2020; 129: 110452.

[2] Khan A, Shal B, Naveed M, Shah FA, Atiq A, Khan NU, *et al*. Matrine ameliorates anxiety and depression-like behaviour by targeting hyperammonemia-induced neuroinflammation and oxidative stress in CCl4 model of liver injury. Neurotoxicology. 2019; 72: 38–50.

[3] Kenda M, Kočevar Glavač N, Nagy M, Sollner Dolenc M. Medicinal Plants Used for Anxiety, Depression, or Stress Treatment: An Update. Molecules. 2022; 27: 6021.

[4] Nuss P, Ferreri F, Bourin M. An update on the anxiolytic and neuroprotective properties of etifoxine: from brain GABA modulation to a whole-body mode of action. Neuropsychiatric Disease and Treatment. 2019; 15: 1781–1795.

[5] Saha D, Paul S. Phytochemical screening and in vitro antioxidant activity of chloroform extract of *Urena sinuata* (L.). International Journal of Pharmaceutical Research and Innovation. 2013; 6: 19–24.

[6] Lans C. Ethnomedicines used in Trinidad and Tobago for reproductive problems. Journal of Ethnobiology and Ethnomedicine. 2007; 3: 13.

[7] Dibyajyoti S, Swati P. Phytochemical Screening and Thrombolytic Activity of Chloroform Extract of *Urena sinuata* (L.). Journal of Fundamental and Applied Sciences. 2014; 6: 208–219.

[8] Sosa A, Rosquete C. Flavonoids from *Urena sinuata* L. Avances en Química. 2010; 5: 95–98.

[9] Mitaine-Offer AC, Sosa A, Rosquete C, Bruno J, Rojas L, Pouységu L, *et al*. Crystal Structure Analysis of 6, 7-Di-O-Methyl-Quercetagetin-3-OBD-Glucopyranoside Dihydrate Isolated from *Urena sinuata* L. Avances en Química. 2011; 6: 55–59.

[10] Uddin MMN, Zahan S, Islam MA, Ahmed S, Rahman MS, Sultan RA, *et al*. Evaluation of the Anti-Diarrheal Activity of Methanol Extract and Its Fractions of *Urena sinuata* L.(Borss)

Leaves. Journal of Applied Pharmaceutical Science. 2016; 6: 56–60.
[11] Mannan A, Sharmin F, Fatema T, Sikder MOF. In Vitro Thrombolytic Assay of *Alpinia zerumbet*, *Alpinia nigra* and *Urena sinuata*. International Journal of Research in Phytochemistry and Pharmacology. 2011; 1: 187–191.
[12] Emran TB, Rahman MA, Uddin MMN, Rahman MM, Uddin MZ, Dash R, *et al*. Effects of organic extracts and their different fractions of five Bangladeshi plants on in vitro thrombolysis. BMC Complementary and Alternative Medicine. 2015; 15: 128.
[13] Abdullah M, Pk AK, Saleh D, Khan AR, Islam N. Insecticidal and Repellent Activities of the Chloroform Extracts of *Urena sinuata* L. against Tribolium Castaneum (Herbst) Adults. University Journal of Zoology, Rajshahi University. 2011; 30: 25–28.
[14] Rahman A, Emran T. Bin Sedative, Anxiolytic and Analgesic Effects of Urena Sinuata L. Leaf Extract in Animal Models. International Food Research Journal. 2014; 21: 2069–2075.
[15] Trease GE, Evans WC. Pharmacognosy. 11th edn. London: Brailliar Tiridel Can. 1989.
[16] Ghani A. Medicinal Plants of Bangladesh, Asiatic Society of Bangladesh. Dhaka, Bangladesh. 2003; 5: e4.
[17] Saeed N, Khan MR, Shabbir M. Antioxidant activity, total phenolic and total flavonoid contents of whole plant extracts *Torilis leptophylla* L. BMC Complementary and Alternative Medicine. 2012; 12: 221.
[18] John B, Sulaiman CT, George S, Reddy VRK. Total Phenolics and Flavonoids in Selected Medicinal Plants from Kerala. International Journal of Pharmacy and Pharmaceutical Sciences. 2014; 6: 406–408.
[19] Manzocco L, Anese M, Nicoli MC. Antioxidant Properties of Tea Extracts as Affected by Processing. LWT-Food Science and Technology. 1998; 31: 694–698.
[20] Marcocci L, Maguire JJ, Droy-Lefaix MT, Packer L. The nitric oxide-scavenging properties of *Ginkgo biloba* extract EGb 761. Biochemical and Biophysical Research Communications. 1994; 201: 748–755.
[21] Ruch RJ, Cheng SJ, Klaunig JE. Prevention of cytotoxicity and inhibition of intercellular communication by antioxidant catechins isolated from Chinese green tea. Carcinogenesis. 1989; 10: 1003–1008.
[22] Sakat S, Juvekar AR, Gambhire MN. In Vitro Antioxidant and Anti-Inflammatory Activity of Methanol Extract of *Oxalis corniculata* Linn. International Journal of Pharmaceutical Sciences Research. 2010; 2: 146–155.
[23] OECD Acute Oral Toxicity – Acute Toxic Class Method 423 Adopted. Guideline for Testing of Chemicals. 2001:1-4.
[24] El Hilaly J, Israili ZH, Lyoussi B. Acute and chronic toxicological studies of *Ajuga iva* in experimental animals. Journal of Ethnopharmacology. 2004; 91: 43–50.
[25] Habib MIB, Rokonuzzman M, Rahman M, Sakib E, Chowdhury MM, Tareq, *et al*. Anti-pyretic effect of methanolic *Physalis micrantha* Link. extract. International Journal of Advanced Biochemistry Research. 2017; 1: 11–13.
[26] Islam MS, Hossain R, Ahmed T, Rahaman MM, Al-Khafaji K, Khan RA, *et al*. Anxiolytic-like Effect of Quercetin Possibly through GABA Receptor Interaction Pathway: In Vivo and In Silico Studies. Molecules. 2022; 27: 7149.
[27] UniProt Consortium. UniProt: a hub for protein information. Nucleic Acids Research. 2015; 43: D204–D212.
[28] Shah N, Nute MG, Warnow T, Pop M. Misunderstood parameter of NCBI BLAST impacts the correctness of bioinformatics workflows. Bioinformatics. 2019; 35: 1613–1614.
[29] Mia MN, Smrity SZ, Bappi MH, Kamli H, Islam T, Prottay AAS, *et al*. Anxiolytic-like effect of succinic acid: A possible GABAergic intervention. Food Bioscience. 2023; 55: 103044.
[30] Wang H, Yao Q, Guo Y, Zhang Q, Wang Z, Strasser RJ, *et al*. Structure-based ligand design and discovery of novel tenuazonic acid derivatives with high herbicidal activity. Journal of Advanced Research. 2022; 40: 29–44.
[31] Abdullahi M, Adeniji SE. In silico molecular docking and ADME/pharmacokinetic prediction studies of some novel carboxamide derivatives as anti-tubercular agents. Chemistry Africa. 2020; 3: 989–1000.
[32] Bappi MH, Prottay AAS, Kamli H, Sonia FA, Mia MN, Akbor MS, *et al*. Quercetin Antagonizes the Sedative Effects of Linalool, Possibly through the GABAergic Interaction Pathway. Molecules. 2023; 28: 5616.
[33] Yuan S, Chan HS, Hu Z. Using PyMOL as a platform for computational drug design. Wiley Interdisciplinary Reviews: Computational Molecular Science. 2017; 7: 1298.
[34] Baroroh U, Biotek M, Muscifa ZS, Destiarani W, Rohmatullah FG, Yusuf M. Molecular interaction analysis and visualization of protein-ligand docking using Biovia Discovery Studio Visualizer. Indonesian Journal of Computational Biology. 2023; 2: 22–30.
[35] Bhuia MS, Kamli H, Islam T, Sonia FA, Kazi MA, Siam MS, *et al*. Antiemetic activity of trans-ferulic acid possibly through muscarinic receptors interaction pathway: In vivo and in silico study. Results in Chemistry. 2023; 6: 101014.
[36] Valanciute A, Nygaard L, Zschach H, Maglegaard Jepsen M, Lindorff-Larsen K, Stein A. Accurate protein stability predictions from homology models. Computational and Structural Biotechnology Journal. 2022; 21: 66–73.
[37] Kim DC, Kang M, Biswas A, Yang CR, Wang X, Gao JX. Effects of low dose ionizing radiation on DNA damage-caused pathways by reverse-phase protein array and Bayesian networks. Journal of Bioinformatics and Computational Biology. 2017; 15: 1750006.
[38] Sharma R, Kumar R, Kodwani R, Kapoor S, Khare A, Bansal R, *et al*. A Review on Mechanisms of Anti-Tumor Activity of Chalcones. Anti-Cancer Agents in Medicinal Chemistry. 2015; 16: 200–211.
[39] Sevcovicova A, Bodnarova K, Loderer D, Imreova P, Galova E, Miadokova E. Dual activities of emodin–DNA protectivity vs mutagenicity. Neuro Endocrinology Letters. 2014; 35: 149–154.
[40] Yuan H, Luo Z, Ban Z, Reiter RJ, Ma Q, Liang Z, *et al*. Bioactive peptides of plant origin: distribution, functionality, and evidence of benefits in food and health. Food & Function. 2022; 13: 3133–3158.
[41] Foti MC. Use and Abuse of the DPPH(•) Radical. Journal of Agricultural and Food Chemistry. 2015; 63: 8765–8776.
[42] Islam M, Prottay AAS, Sultana I, Al Faruq A, Bappi MH, Islam MT, *et al*. Phytochemical screening and evaluation of antioxidant, anti-inflammatory, antimicrobial, and membrane-stabilizing activities of different fractional extracts of *Grewia nervosa* (Lour.) Panigrahi. Food Bioscience. 2023; 54: 102933.
[43] Kaur IP, Geetha T. Screening methods for antioxidants-a review. Mini Reviews in Medicinal Chemistry. 2006; 6: 305–312.
[44] Bhuia MS, Rahaman MM, Islam T, Bappi MH, Sikder MI, Hossain KN, *et al*. Neurobiological effects of gallic acid: current perspectives. Chinese Medicine. 2023; 18: 27.
[45] Juee LY, Sofi SH, Adham AN. *Melissa officinalis* gastroprotective and antioxidant efficacy. Journal of Functional Foods. 2023; 105: 105550.
[46] Mondal A, Maity TK, Bishayee A. Analgesic and Anti-Inflammatory Activities of Quercetin-3-methoxy-4'-glucosyl-7-glucoside Isolated from Indian Medicinal Plant *Melothria heterophylla*. Medicines. 2019; 6: 59.
[47] Adhikari B. Roles of alkaloids from medicinal plants in the management of diabetes mellitus. Journal of Chemistry. 2021; 2021: 1–10.

Journal of
BIOLOGICAL REGULATORS
and Homeostatic Agents

[48] da Silva MG, Daros GC, de Bitencourt RM. Anti-inflammatory activity of ayahuasca: therapeutical implications in neurological and psychiatric diseases. Behavioural Brain Research. 2021; 400: 113003.

[49] Zaman F, Sarkar C, Hossain R, Molla S, Das AK, Shuvo APR, *et al*. Phytochemical Evaluation and Pharmacological Activities of Blume Leaf Extract. Acta Biologica Marisiensis. 2022; 5: 1–16.

[50] Costa JP, de Oliveira GAL, de Almeida AAC, Islam MT, de Sousa DP, de Freitas RM. Anxiolytic-like effects of phytol: possible involvement of GABAergic transmission. Brain Research. 2014; 1547: 34–42.

[51] Hossain R, Al-Khafaji K, Khan RA, Sarkar C, Islam MS, Dey D, *et al*. Quercetin and/or Ascorbic Acid Modulatory Effect on Phenobarbital-Induced Sleeping Mice Possibly through GABA_*A* and GABA_*B* Receptor Interaction Pathway. Pharmaceuticals. 2021; 14: 721.

[52] Peirce JM, Alviña K. The role of inflammation and the gut microbiome in depression and anxiety. Journal of Neuroscience Research. 2019; 97: 1223–1241.

[53] Islam MS, Quispe C, Hossain R, Islam MT, Al-Harrasi A, Al-Rawahi A, *et al*. Neuropharmacological Effects of Quercetin: A Literature-Based Review. Frontiers in Pharmacology. 2021; 12: 665031.

[54] Emran T, Ahmed S, Zahan S, Rakib A, Hasan M, Amin M, *et al*. Sedative, Anxiolytic, Antinociceptive, Anti-Inflammatory, and Antipyretic Effects of a Chloroform Extract from the Leaves of *Urena sinuata* in Rodents. Journal of Applied Life Sciences International. 2018; 16: 1–19.

[55] Yang L, Wang ZM, Wang Y, Li RS, Wang F, Wang K. Phenolic constituents with neuroprotective activities from *Hypericum wightianum*. Phytochemistry. 2019; 165: 112049.

[56] López JGE. Flavonoids in Health and Disease. Current Medicinal Chemistry. 2019; 26: 6972–6975.

[57] Patel L, Shukla T, Huang X, Ussery DW, Wang S. Machine Learning Methods in Drug Discovery. Molecules. 2020; 25: 5277.

[58] Peng Y, Cheng Z, Xie F. Evaluation of Pharmacokinetic Drug-Drug Interactions: A Review of the Mechanisms, In Vitro and In Silico Approaches. Metabolites. 2021; 11: 75.

[59] Lee S, Suh YJ, Yang S, Hong DG, Ishigami A, Kim H, *et al*. Neuroprotective and Anti-Inflammatory Effects of Evernic Acid in an MPTP-Induced Parkinson's Disease Model. International Journal of Molecular Sciences. 2021; 22: 2098.

[60] Hong DG, Lee S, Kim J, Yang S, Lee M, Ahn J, *et al*. Anti-Inflammatory and Neuroprotective Effects of Morin in an MPTP-Induced Parkinson's Disease Model. International Journal of Molecular Sciences. 2022; 23: 10578.

[61] Singh D, Hembrom S, Raj A. Neuroprotective effect of flavonoids: A systematic review. Journal of Pharmacognosy and Phytochemistry. 2019; 8: 699–707.

[62] Bhuia MS, Wilairatana P, Ferdous J, Chowdhury R, Bappi MH, Rahman MA, *et al*. Hirsutine, an Emerging Natural Product with Promising Therapeutic Benefits: A Systematic Review. Molecules. 2023; 28: 6141.

[63] She Y, Shao L, Zhang Y, Hao Y, Cai Y, Cheng Z, *et al*. Neuroprotective effect of glycosides in Buyang Huanwu Decoction on pyroptosis following cerebral ischemia-reperfusion injury in rats. Journal of Ethnopharmacology. 2019; 242: 112051.

[64] Long S, Resende DISP, Kijjoa A, Silva AMS, Fernandes R, Xavier CPR, *et al*. Synthesis of New Proteomimetic Quinazolinone Alkaloids and Evaluation of Their Neuroprotective and Antitumor Effects. Molecules. 2019; 24: 534.

[65] An J, Chen B, Kang X, Zhang R, Guo Y, Zhao J, *et al*. Neuroprotective effects of natural compounds on LPS-induced inflammatory responses in microglia. American Journal of Translational Research. 2020; 12: 2353–2378.